Monte Carlo Modeling and Simulation of Electron Dynamics in Low Temperature Methane Gas

Abdelatif Gadoum
LRPPS Laboratory, Faculty of Mathematics and Material Sciences, Kasdi Merbah Ouargla University, Algeria | Electrical Engineering and Renewable Energies Laboratory, Chlef University, Algeria
gdabdelatif@gmail.com (corresponding author)

Djilali Benyoucef
Electrical Engineering and Renewable Energies Laboratory, Chlef University, Algeria
d.benyoucef@univ-chlef.dz

Received: 12 August 2024 | Revised: 18 September 2024 | Accepted: 4 October 2024

 DOI: https://doi.org/10.48084/etasr.8712

ABSTRACT

This study examines the collisions of electrons with methane molecules to determine the cross-sections required for calculating electron transport coefficients in methane gas. Employing Monte Carlo Simulations in MATLAB, critical transport characteristics, including electron mobility and diffusion coefficients, were computed. These simulated coefficients are subsequently compared to experimental data to validate the accuracy of the current study's findings. This comprehensive approach ensures the precision of the performed calculations and their alignment with empirical evidence, thereby enhancing the understanding of the complex interactions and dynamics between electrons and methane molecules in this system.

Keywords-monte carlo simulation; electron transport coefficients; electron-methane collision; low-temperature physics; gas discharge modeling

I. INTRODUCTION

Plasma discharge modeling is essential as it provides insights into the complex interactions and behaviors of the charged and neutral particles within the plasma [1, 2]. This understanding is vital for optimizing plasma-based processes, predicting their outcomes, and improving the design and efficiency of plasma technologies used in various fields, such as material processing, environmental control, and electronics [3-6]. Plasma discharge modeling requires a comprehensive understanding of all the physical processes occurring between electrons and the background gas molecules or atoms [7-10]. These processes encompass ionization, excitation, attachment, recombination, dissociation, and elastic collisions [11, 12]. The probabilities of these physical processes are defined by their respective cross-sections, which can be used to calculate the Electron Energy Distribution Function (EEDF) and the electron transport coefficients. However, the current research often lacks a comprehensive dataset of cross-sections for electron-methane collisions, limiting the understanding of the fundamental interactions and their applications. By developing a complete set of cross-sections, this knowledge gap can be bridged, providing critical insights into the behavior of methane in diverse environments, ranging from industrial processes to extraterrestrial atmospheres. These data are crucial for improving plasma models, advancing technologies like gas discharge lamps, and ensuring safety in environments where methane is present. Additionally, accurate cross-sections are essential for validating theoretical models and enhancing simulations in both experimental and practical contexts.

This study investigates methane (CH_4) and the relevant data required to reproduce its transport coefficients based on experimental measurements. The literature has extensively explored the determination of electron transport coefficients in pure methane and mixtures, typically with hydrogen (H_2). These gas mixtures are essential in various material processing applications, including the etching of indium phosphide, diamond deposition and coating, as well as the optoelectronics and communication industries for the manufacture of devices such as solar cells and laser diodes [13-15].

Furthermore, this study utilizes the Monte Carlo Simulation Method to calculate the electron mobility, transverse diffusion coefficient, and ionization coefficient in methane. This indirect approach is based on the laws that solve the Boltzmann equation [16, 17]. Previous work employed a pulsed drift tube to measure electron drift velocity in methane from 10 to 1000 Td, as well as positive ion mobility and ionization coefficient from 80 to 1000 Td [18]. No evidence of attachment was observed within this range. The Monte Carlo Simulations,

which incorporated a comprehensive set of collision cross sections covering momentum transfer, vibrational excitation, ionization, and dissociation into neutrals, demonstrated excellent agreement with the experimental swarm parameters, enabling accurate results without the need for adjustments.

In contrast, predictions using the two-term Boltzmann equation with the same cross sections were found to be inaccurate, highlighting the limitations of this method for modeling methane. An enhanced pulsed Townsend technique was employed to measure electron transport parameters in gases [19]. The accuracy of this technique was validated by measuring electron attachment coefficients in oxygen and drift velocities in methane across a broad range of *E*/*N* values. The measurements exhibit good agreement with existing data and demonstrate that the technique can precisely quantify electron attachment coefficients in methane, which can be significantly smaller than ionization coefficients, up to a factor of 10. The results are consistent with Boltzmann equation analyses utilizing published scattering cross sections.

A novel technique enabling the precise measurement of both electron drift velocity and diffusion coefficients in a single experiment was developed in [20]. This method provides direct measurements without the need for boundary corrections, making it well-suited for determining scattering cross sections. Utilizing a proportional counter for single-electron detection, the technique proves particularly effective in investigations of hydrocarbon gases. Furthermore, another study explored electron diffusion in various gases under a uniform electric field, allowing them to determine key transport parameters, such as electron drift velocity, diffusion coefficients, and their ratios [21]. Analyzing the lateral spread of electron streams helped infer the average kinetic energy of the electrons and calculate the mean free path, energy loss per collision, and gas kinetic cross section. This research builds upon previous studies by examining a broader range of gases and experimental conditions, including *E*/*P* ratios from 0.2 to 5.0 (V/cm)/(mm.Hg), providing valuable insights into the behavior of low-energy electrons in different gas environments.

Authors in [22] investigated electron swarm properties in methane, silane, phosphine, and hydrogen sulfide using a modified pulsed Townsend technique [22]. Improvements in the experimental setup are detailed, including enhanced gas purification and a microcomputer-based data system, to measure electron drift and diffusion characteristics accurately across various pressures and *E*/*N* values. Authors in [23] expanded previous electron swarm studies by measuring the ionization coefficient, drift velocity, and diffusion coefficients across a variety of gases. They enhanced the accuracy of their findings by addressing secondary electron effects and implementing computerized data analysis to obtain new *Dr*/*p* values for gases, including helium, argon, air, methane, and nitric oxide, thereby expanding the range of gases studied. Separately, a different study utilized a pulsed Townsend technique to measure ionization coefficients, electron drift velocities, and positive ion drift velocities in methane-argon mixtures across an *E*/*N* range from 0.05×10^{-17} to 700×10^{-17} V.cm^2, with mixture ratios varying from 0.5 to 75% methane [24]. Their results showed that at low *E*/*N*, the ionization coefficient depended on methane concentration, but converged at higher *E*/*N*. The electron drift velocities exhibited a distinct negative differential conductivity region, with the locations of maxima and minima shifting according to the methane content. Additionally, electron swarm properties in methane, silane, phosphine, and hydrogen sulfide were investigated using a modified pulsed Townsend technique. Their work detailed improvements to the experimental setup, including enhanced gas purification and a microcomputer-based data system, were detailed to accurately measure electron drift and diffusion characteristics across various pressures and *E*/*N* values.

II. ELECTRON COLLISON CROSS SECTIONS WITH METHANE

The electron collision cross sections with methane molecules are physical quantities related to the probability of electron-methane interactions for various reaction processes, involving ionization, excitation, attachment, recombination, dissociation, and elastic collisions. These quantities can be determined through two distinct methods: direct measurement and deconvolution employing transport coefficient measurements [25]. The collision processes between methane molecules and electron impact, along with their associated energy thresholds, are listed in Table I [26-29]. The reaction outlined in Table I represents momentum transfer, and its cross section provides a measure of the momentum exchange during an elastic collision, which can be calculated using:

$$\sigma_1(\varepsilon) = 2\pi \int_0^{\pi} \frac{d\sigma_{el}(\varepsilon,\chi)}{d\chi} \sin(\chi)\left(1-\cos(\chi)\right) d\chi \quad (1)$$

where $\sigma 1(\varepsilon)$ and $\sigma_{el}(\varepsilon,\chi)$ are the momentum and the elastic cross section, respectively, ε and χ are the electron energy and the diffusion angle, respectively. The continuous line in Figure 1 represents the fitted data of the measurements from various studies [30-37].

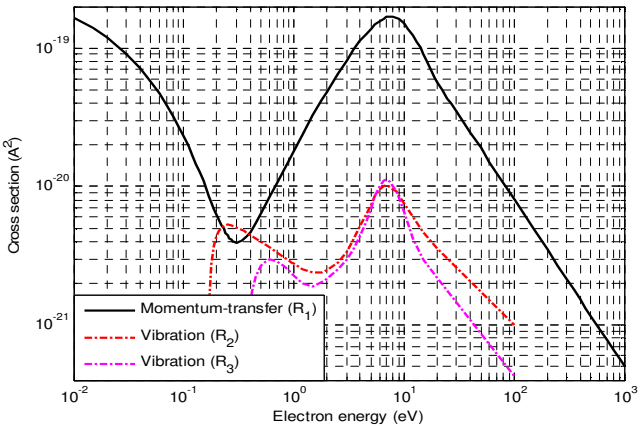

Fig. 1. Electron methane molecule cross section: Momentum transfer cross section (continuous line) and vibration cross sections (dashed lines).

The reactions, R2 and R3, represent the vibration processes of methane molecule due to the electron impact collision; their cross sections are represented by dashed lines in Figure 1, taking into account the measurements of a number of research studies [38-40].

The partial ionization cross-sections of the relevant reactions, R8 through R14, used in this study are already measured and normalized to the total ionization cross-sections [41, 42]. The excited states of methane are short-lived, resulting in the dissociation of all excited molecules into fragments [18, 43]. In addition to the total dissociative cross-section into neutral fragments and neutral ion fragments, the literature also provides the measured cross-sections for the production of CH_3, corresponding to reactions R4 and R14 given in Table I [44, 45]. The interpolation of these data is shown in Figure 2 as a continuous line.

TABLE I. ELECTRON IMPACT COLLISIONS WITH METHANE MOLECULE

Symbol	Collision Processes	Threshold (eV)	Nature Of Reaction
R_1	$e+CH_4 => e + CH_4$	-	Elastic Collision
R_2	$e+CH_4 => e + CH_4$	0.162	
R_3	$e+CH_4 => e + CH_4$	0.362	
R_4	$e+CH_4 => e + CH_3 + H$	8.8	Partial Dissociation
R_5	$e+CH_4 => e + CH_2 + H_2$	9.4	
R_6	$e+CH_4 => e + CH + H_2 + H$	12.5	
R_7	$e+CH_4 => e + C + 2H_2$	14	
R_8	$e+CH_4 => 2e + CH_4^+$	12.63	Partial Ionization
R_9	$e+CH_4 => 2e + CH_3^+ + H$	14.25	
R_{10}	$e+CH_4 => 2e + CH_2^+ + H_2$	15.1	
R_{11}	$e+CH_4 => 2e+CH^+ + H_2 + H$	19.9	
R_{12}	$e+CH_4 => 2e + C^+ + 2H_2$	19.6	
R_{13}	$e+CH_4 => 2e + H_2^+ + CH_2$	20.1	
R_{14}	$e+CH_4 => 2e + H^+ + CH_3$	18.0	

For the calculation of the different partial dissociative cross-sections σ_4, σ_5, σ_6, and σ_7 of the reactions R4, R5, R6, and R7, respectively, it is necessary to calculate the total dissociative cross section into neutrals σ_{nd} by:

$$\begin{cases} \sigma_{\mathrm{nd}} = \dfrac{\sigma_4}{\sigma_9 + \sigma_{14}} \sigma_{\mathrm{id}} \\ \sigma_{\mathrm{CH_3}} = \sigma_4 + \sigma_{14} \end{cases} \quad (2)$$

where σ_{CH_3} is the cross-section of CH_3 production ($\sigma_4+\sigma_{14}$), σ_{14} is the cross-section of the reaction R14, σ_{id} represents the total cross section for all dissociative processes into neutral fragments. The cross section of the reactions R5, R6, and R7 can be calculated utilizing:

$$\begin{cases} \sigma_5 = \dfrac{\sigma_{\mathrm{nd}}}{\sigma_{\mathrm{id}}} \left(\sigma_{10} + \sigma_{13} \right) \\ \sigma_6 = \dfrac{\sigma_{\mathrm{nd}}}{\sigma_{\mathrm{id}}} \sigma_{11} \\ \sigma_7 = \dfrac{\sigma_{\mathrm{nd}}}{\sigma_{\mathrm{id}}} \sigma_{12} \end{cases} \quad (3)$$

where σ_{10}, σ_{11}, σ_{12}, and σ_{13} are the cross sections of the reactions R10, R11, R12, and R13, respectively. The total dissociative cross section into neutrals and the total ionization cross section are portrayed in Figure 2.

Figure 1 depicts the cross-sectional data for electron-methane collisions, entailing the momentum transfer cross-section and vibration cross-sections. The momentum transfer cross-section decreases as electron energy increases, indicating a reduced momentum exchange between electrons and methane. Conversely, the vibration cross-sections display distinct peaks at specific energies, signifying the resonant excitation of vibrational modes in methane. Figure 1 elucidates how different collision processes prevail at varying energy levels, offering essential insights for plasma physics applications and the validation of theoretical models.

The vibrational cross-sections frequently display pronounced peaks at particular electron energies. These peaks signify the resonant excitation of vibrational modes within the methane molecule. The location and amplitude of these peaks offer valuable insights into the vibrational energy levels of methane and the effectiveness of vibrational excitation processes.

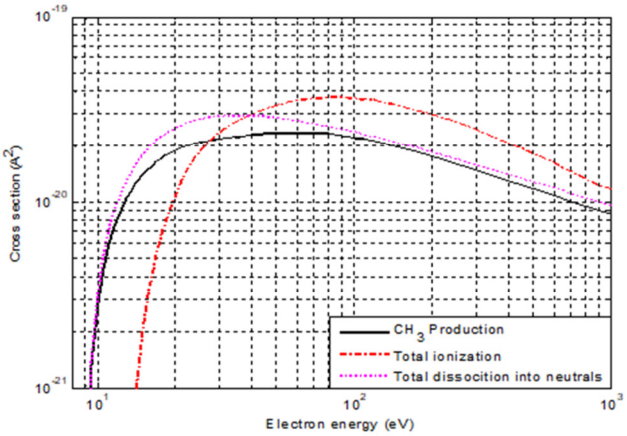

Fig. 2. Electron methane molecule cross section: CH_3 production (continuous line), total ionization (dashed line), and total dissociation into neutrals (dotted line).

The analysis of the various cross sections for electron collisions with methane reveals important insights. The CH_3 production cross section demonstrates specific energy ranges, where electron collisions generate CH_3 radicals more effectively, highlighting the energy-dependent nature of these production rates. Similarly, the total ionization cross section increases with electron energy, indicating higher probabilities of ionization at elevated energies. In contrast, the total dissociation cross section exhibits a more complex pattern, with potential peaks at certain energies, reflecting the varied efficiencies of the dissociation process. Figure 2 provides valuable information for optimizing methane-based processes and validating theoretical models by illustrating how different collision processes are influenced by electron energy.

III. TRANSPORT COEFFICIENTS CALCULATION BY MONTE CARLO SIMULATION

The electron transport coefficients are crucial in the field of plasma modeling. These coefficients can be calculated by solving the Boltzmann equation, which can be approached using two distinct methods: the analytic method based on the development in Legendre polynomials, and the stochastic method known as the Monte Carlo Simulation Method [11, 12, 17, 46-48]. The latter is founded on the processing of a sample of electrons, tracking their movements in the phase space by integrating the equations of motion and considering the effect of the applied electromagnetic force. In the case where an electron undergoes K types of collisions, the collision frequency ν is a function of the neutral density N, the total cross-section $\sigma_T(\varepsilon)$, and the electron energy ε, as presented in:

$$\upsilon(\varepsilon) = N.\sigma_T(\varepsilon).\sqrt{\frac{2\varepsilon}{m_e}} \quad (4)$$

where m_e is the electron mass. The collision probability $p(t_v)$ after a flight time t_v is given by:

$$p(t_v) = 1 - \exp(-\int_0^{t_v} \upsilon_T(\varepsilon)dt) \quad (5)$$

To determine the free flight time, it is necessary to integrate the governing equation, which in the general case lacks an analytical solution. To optimize the computation times, this study introduces the concept of a zero collision, corresponding to an additional frequency selected, such that the total collision frequency remains constant regardless of the energy. This constant is typically equal to the actual maximum total collision frequency, υ_{max}, and the free flight time is expressed by:

$$\upsilon_{\max} = N.\max\left\{\sum_{i=1}^{K} \sigma_i(\varepsilon).\sqrt{\frac{2\varepsilon}{m_e}}\right\}$$
$$t_{vol} = -\frac{\ln(1-R_{vol})}{\upsilon_{\max}} \quad (6)$$

where R_{vol} is a random number uniformly distributed between 0 and 1. The probability fraction of each type of collision, with υ_i frequency, is given by:

$$p_i = \frac{\upsilon_i}{\upsilon_{\max}} \quad (7)$$

Following each real collision, the scattering angles, axial χ and azimuthal ψ, are determined by the straightforward generation of two randomly distributed uniform numbers, $R\chi$ and $R\psi$, between 0 and 1. Furthermore, in the case of an elastic collision, the electron energy loss is given by the subsequent expression:

$$\Delta\varepsilon = 2\frac{m_e}{M}(1-\cos\chi)\varepsilon$$
$$\psi = 2\pi R_\psi, \chi = \operatorname{acos}(1 - 2R_\chi) \quad (8)$$

In the case of an inelastic collision, the electron energy decreases by an amount corresponding to the threshold energy of the collision. During ionization, an electron-ion pair is created, and the remaining energy is distributed between the ejected electron and the newly formed electron. At the start of the simulation, all electrons are considered to have a uniform initial energy at the given location, with x, y, and z being equal to zero. The electrons then move under the influence of a uniform electric field applied in the opposite direction of the z-axis. After a sufficient simulation time, t_s, the average electron energy stabilizes at which point the transport coefficients can be evaluated using the average values calculated from t_s to the final simulation time, t_f:

$$\mu_e = \frac{z(t_f)-z(t_s)}{|E|(t_f-t_s)}$$
$$D_e = \frac{\left(x(t_f)-x(t_s)\right)^2+\left(y(t_f)-y(t_s)\right)^2}{4(t_f-t_s)} \quad (9)$$
$$\alpha = \frac{\ln\left(\left(\frac{n_0+\Delta n}{n_0}\right)+1\right)}{z(t_f)-z(t_s)}$$

where n_0 receives the value of 10^7 cm^{-3} and Δn are the electron number at the time t_s and the electron number variation from t_s to t_f, respectively.

The Monte Carlo Simulation method for solving the Boltzmann equation involves simulating the movement and interactions of individual particles, updating their positions and velocities based on electric fields and collision events, and calculating transport coefficients from the resulting trajectories. This approach provides detailed insights into the behavior of electrons in various gases through probabilistic modeling and statistical analysis.

Under the influence of an electric field, electrons are accelerated by the energy imparted. Subsequently, after a series of collisions, the electrons reach a steady-state velocity. This equilibrium occurs because the energy gained from the electric field is balanced by the energy lost through collisions. The time parameter t_f equals 0.04 ms, and the time parameter t_s is related to the response time tr for each value of the electrical field, as depicted in Figure 3. The Boltzmann equation for electrons in a gas is given by:

$$\frac{\partial f(r,v,t)}{\partial t} + v.\nabla r f(r,v,t) +$$
$$\frac{eE(r,t)}{m_e}.\nabla_v f(r,v,t) = \left(\frac{\partial f}{\partial t}\right)_{coll} \quad (10)$$

where $f(r, v, t)$ is the distribution function of electrons, which depends on position r, velocity v, and time t, V is the velocity of the electrons, $E(r, t)$ is the electric field, e is the electron's charge, m_e is the mass of the electron, and $\left(\frac{\partial f}{\partial t}\right)_{coll}$ represents the collision term, which includes the effects of collisions between electrons and molecules.

In Monte Carlo Simulation of particle trajectories, the position and velocity updates are given by:

$$r(t+\Delta t) = r(t) + v(t)\Delta t \quad (11)$$

$$v(t+\Delta t) = v(t) + \frac{eE(r(t),t)}{m_e}\Delta t \quad (12)$$

Regarding collision modeling, the collision probability is given by (13), where $\sigma(v)$ is the collision cross-section as a function of velocity v, and n is the number density of target molecules:

$$P_{coll} = 1 - \exp(-\sigma(v)n\Delta t) \quad (13)$$

Equation (14) describes the mean free path:

$$\lambda = \frac{1}{n\sigma(v)} \quad (14)$$

The velocity after a collision is updated according to the type of collision:

$$v' = v + \Delta v_{collision} \quad (15)$$

where $\Delta v_{collision}$ depends on the collision process, such as elastic and inelastic. Choosing the time step size Δt is critical for simulation accuracy and (16) must be satisfied, where v_{max} is the maximum velocity of the particles:

$$\Delta t \leq \frac{\lambda}{v_{\max}} \quad (16)$$

This criterion ensures that particles do not travel too far in a single time step, which would otherwise lead to inaccuracies in collision modeling.

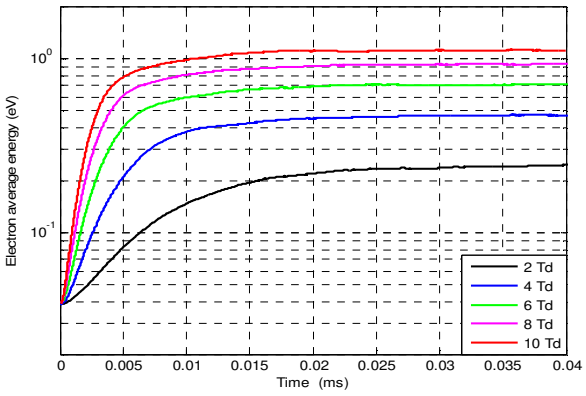

Fig. 3. Comparison between the calculated and measured electron energy evolution as a function of time.

Figure 3 illustrates the evolution of the electron energy as a function of time. It is evident that the time required for the stabilization of the average electron energy increases with the rising reduced electric field *E*/*N*. Figures 4-6 also present a comparison between the calculated and measured transport coefficients of electrons in methane, and the good agreement between them validates the selected cross sections for the different collisional processes employed in this study [18-23]. Moreover, Figure 3 depicts the temporal evolution of electron energy, demonstrating that the time needed for electrons to reach their average energy increases as the reduced electric field *E*/*N* is elevated. This trend suggests that higher electric fields result in a longer equilibration period, which reflects the augmented complexity of electron interactions and energy transfers within more intense electric fields. Similarly, Figure 4 compares the simulated and measured transport coefficients $\mu.N$ for electrons in methane across diverse reduced electric fields *E*/*N*.

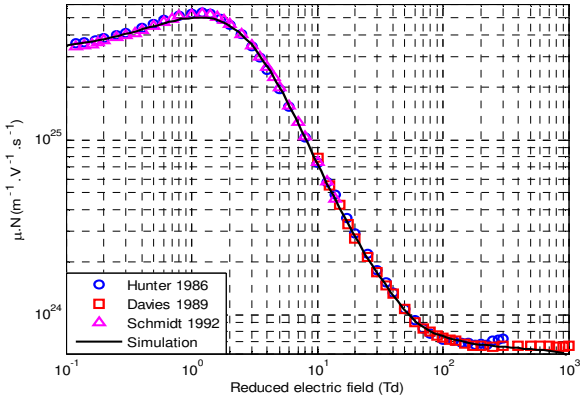

Fig. 4. Comparison between the calculated and the measured u.N ($m^{-1}.V^{-1}.s^{-1}$) in function of reduced electric field.

The strong agreement between the present study's simulation findings and experimental data corroborates the validity of the cross-sectional data employed. Significantly, the results align closely with [19] which utilized a pulsed drift tube to measure drift velocity and other parameters in methane, as well as with the enhanced pulsed Townsend technique described in [42] and the comprehensive measurement approach presented in [43]. This consistent concordance across diverse experimental methodologies and investigations affirms the accuracy of the presented transport coefficient modeling and the reliability of the simulation findings in characterizing electron behavior in methane under varying electric fields.

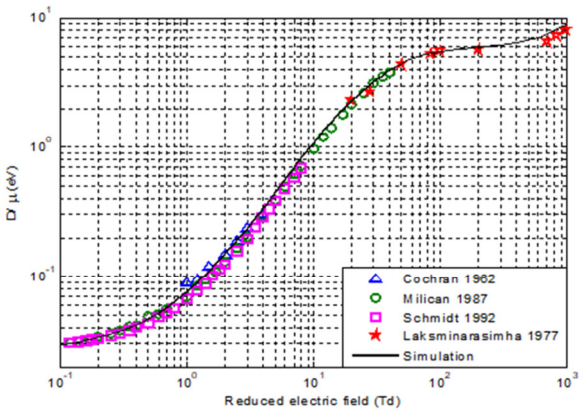

Fig. 5. Comparison between the calculated and the measured D/μ (eV) in function of reduced electric field.

The simulation results, illustrated in Figure 5, are in close agreement with experimentally measured values of the diffusion coefficient to mobility ratio (D/μ) as a function of the reduced electric field (*E*/*N*) for electron collisions in methane. This alignment between the present study's calculated data and the experimental findings reported in prior studies validates the accuracy of the current paper's cross-sectional data and confirms the robustness of the simulation model [20-22, 24].

The observed strong correlation emphasizes the reliability of the proposed methodology in forecasting the ratio of diffusion to mobility across diverse electric field conditions.

This underscores the efficacy of the introduced techniques and cross-sectional data in capturing the core electron transport characteristics in methane.

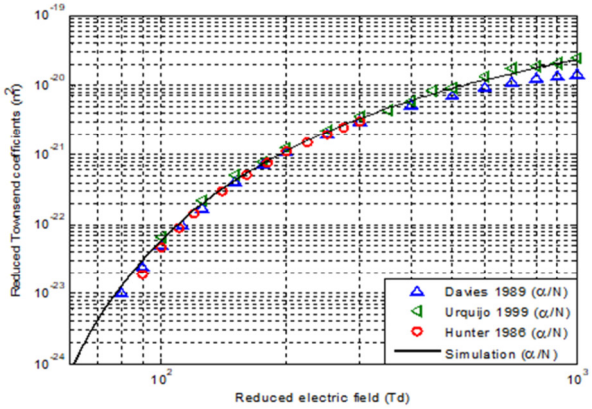

Fig. 6. Comparison between the calculated and the measured Reduced Townsend Coefficient in function of reduced electric field.

The reduced Townsend coefficient as a function of the reduced electric field is compared to data from multiple studies, as evidenced in Figure 6. The close alignment between this study's simulation results and the experimental findings of [18] confirms the accuracy of the proposed cross-sectional data and model.

The present paper demonstrates good correspondence between the presented results and Monte Carlo Simulations, while also highlighting the limitations of two-term Boltzmann methods for modeling methane. Furthermore, authors in [19] validated the effectiveness of an enhanced pulsed Townsend technique for measuring electron transport parameters, corroborating the findings of the current study through consistent values for electron attachment coefficients. Notably, it was reported that methane-argon mixtures aligns well with the predictions of this study, revealing a dependency of ionization coefficients on methane concentration and a negative differential conductivity region in electron drift velocities [24].

The consistent results obtained across diverse experimental conditions and gas compositions emphasize the robustness and precision of the performed simulations in forecasting Townsend ionization coefficients for a range of electric field strengths.

IV. CONCLUSIONS

This study generated a comprehensive set of cross-section data for various collision processes involving electrons and methane molecules. This work is essential, as it provides a robust dataset that enhances our understanding and modeling capabilities regarding electron-methane interactions, particularly under low-temperature conditions, where these interactions are significant. The current study validated this dataset by comparing it with the electron transport coefficients, which were accurately calculated using the Monte Carlo Simulation Method. This method has proven to be an exceptionally powerful and reliable tool for solving the Boltzmann equation, a crucial component for describing the statistical behavior of electrons in the gas phase. By supplying validated data and employing a robust simulation approach, the present work advances both the theoretical and practical models of electron dynamics in gases. This has potential applications across diverse fields, including plasma physics and material chemistry, where a precise understanding of electron interactions is crucial for research and application.

REFERENCES

[1] L. Jr. Spitzer, *Physics of Fully Ionized Gases*, 2nd ed. New York, USA: Dover Publications Inc., 2006.

[2] F. F. Chen, *Introduction to Plasma Physics and Controlled Fusion*. Los Angeles, USA: Springer International Publishing, 2016.

[3] M. Hamidieh and M. Ghassemi, "Theory and Finite-Element Simulation Methodology of Gas Discharge Plasmas," *IEEE Access*, vol. 12, pp. 104688–104707, 2024, https://doi.org/10.1109/ACCESS.2024.3435971.

[4] D. Vu, "Prediction of the Adhesion Strength of Coating in Plasma Spray Deposition," *Engineering, Technology & Applied Science Research*, vol. 13, no. 2, pp. 10367–10371, Apr. 2023, https://doi.org/10.48084/etasr.5673.

[5] D. B. Graves *et al.*, "Science challenges and research opportunities for plasma applications in microelectronics," *Journal of Vacuum Science and Technology B*, vol. 42, no. 4, Jul. 2024, https://doi.org/10.1116/6.0003531.

[6] P. Lamichhane *et al.*, "Critical review: 'Green' ethylene production through emerging technologies, with a focus on plasma catalysis," *Renewable and Sustainable Energy Reviews*, vol. 189, Jan. 2024, Art. no. 114044, https://doi.org/10.1016/j.rser.2023.114044.

[7] B. Parent and F. M. Rodriguez Fuentes, "Progress in electron energy modeling for plasma flows and discharges," *Physics of Fluids*, vol. 36, no. 8, , Aug. 2024 Art. no. 086113, https://doi.org/10.1063/5.0219552.

[8] E. C. Romao, A. F. Siqueira, and J. A. Martins, "Numerical Simulation and Optimization of Methane Steam Reforming to Maximize H2 Production: A Case Study," *Engineering, Technology & Applied Science Research*, vol. 13, no. 2, pp. 10255–10260, Apr. 2023, https://doi.org/10.48084/etasr.5632.

[9] A. Lifa, S. Dilmi, and S. E. Bentridi, "The Influence of Hot Electrons on the Calculation of Ionization Rates," *Engineering, Technology & Applied Science Research*, vol. 12, no. 6, pp. 9579–9583, Dec. 2022, https://doi.org/10.48084/etasr.5294.

[10] S. Dilmi, F. Khalfaoui, and A. Boumali, "The Effects of Superstatistics Properties on Hot Plasma," *Engineering, Technology & Applied Science Research*, vol. 12, no. 5, pp. 9342–9346, Oct. 2022, https://doi.org/10.48084/etasr.5223.

[11] D. Benyoucef and M. Yousfi, "Particle modelling of magnetically confined oxygen plasma in low pressure radio frequency discharge," *Physics of Plasmas*, vol. 22, no. 1, Jan. 2015, Art. no. 013510, https://doi.org/10.1063/1.4907178.

[12] M. Mostafaoui and D. Benyoucef, "Electrical model parameters identification of radiofrequency discharge in argon through 1D3V/PIC-MC model," *Plasma Science and Technology*, vol. 20, no. 9, pp. 95401–095401, 2018, https://doi.org/10.1088/2058-6272/aac3cf.

[13] J. S. Yu and Y. T. Lee, "Reactive ion etching of InP for optoelectronic device applications: Comparison in CH4, CH4/H2, and CH4/Ar gas," *Journal of the Korean Physical Society*, vol. 37, pp. 241–246, Sep. 2000.

[14] H. Sein *et al.*, "Chemical vapour deposition diamond coating on tungsten carbide dental cutting tools," *Journal of Physics: Condensed Matter*, vol. 15, no. 39, Jun. 2003, https://doi.org/10.1088/0953-8984/15/39/019.

[15] M. O. Manasreh, Ed., InP and Related Compounds: Materials, Applications and Devices. London, UK: CRC Press, 2014.

[16] D. Benyoucef, "Modélisation particulaire et multidimensionnelle des décharges hors équilibre à basse pression excitées par champs électromagnétiques," Université de Toulouse, Toulouse, France, 2011.

[17] D. Benyoucef, M. Yousfi, B. Belmadani, and A. Settaouti, "PIC MC Using Free Path for the Simulation of Low-Pressure RF Discharge in

Argon," *IEEE Transactions on Plasma Science*, vol. 38, no. 4, pp. 902–908, Apr. 2010, https://doi.org/10.1109/TPS.2010.2042305.

[18] D. K. Davies, L. E. Kline, and W. E. Bies, "Measurements of swarm parameters and derived electron collision cross sections in methane," *Journal of Applied Physics*, vol. 65, no. 9, pp. 3311–3323, May 1989, https://doi.org/10.1063/1.342642.

[19] S. R. Hunter, J. G. Carter, and L. G. Christophorou, "Electron transport measurements in methane using an improved pulsed Townsend technique," *Journal of Applied Physics*, vol. 60, no. 1, pp. 24–35, Jul. 1986, https://doi.org/10.1063/1.337690.

[20] B. Schmidt and M. Roncossek, "Drift velocity, longitudinal and transverse diffusion in hydrocarbons derived from distributions of single electrons," *Australian Journal of Physics*, vol. 45, Jan. 1992, Art. no. 351, https://doi.org/10.1071/PH920351.

[21] L. W. Cochran and D. W. Forester, "Diffusion of Slow Electrons in Gases," *Physical Review*, vol. 126, no. 5, pp. 1785–1788, Jun. 1962, https://doi.org/10.1103/PhysRev.126.1785.

[22] P. G. Millican and I. C. Walker, "Electron swarm characteristic energies (Dr/μ) in methane, perdeuteromethane, silane, perdeuterosilane, phosphine and hydrogen sulphide at low E/N," *Journal of Physics D: Applied Physics*, vol. 20, no. 2, Oct. 1987, Art. no. 193, https://doi.org/10.1088/0022-3727/20/2/007.

[23] C. S. Lakshminarasimha and J. Lucas, "The ratio of radial diffusion coefficient to mobility for electrons in helium, argon, air, methane and nitric oxide," *Journal of Physics D: Applied Physics*, vol. 10, no. 3, Oct. 1977, Art. no. 313, https://doi.org/10.1088/0022-3727/10/3/011.

[24] J. de Urquijo, I. Alvarez, E. Basurto, and C. Cisneros, "Measurement of ionization and electron transport in methane-argon mixtures," *Journal of Physics D: Applied Physics*, vol. 32, no. 14, Apr. 1999, Art. no. 1646, https://doi.org/10.1088/0022-3727/32/14/316.

[25] T. Sakae, S. Sumiyoshi, E. Murakami, Y. Matsumoto, K. Ishibashi, and A. Katase, "Scattering of electrons by CH4, CF4 and SF 6 in the 75-700 eV range," *Journal of Physics B: Atomic, Molecular and Optical Physics*, vol. 22, no. 9, pp. 1385–1394, 1989, https://doi.org/10.1088/0953-4075/22/9/011.

[26] R. K. Janev and D. Reiter, "Collision processes of CHy and CHy+ hydrocarbons with plasma electrons and protons," *Physics of Plasmas*, vol. 9, no. 9, pp. 4071–4081, Sep. 2002, https://doi.org/10.1063/1.1500735.

[27] M.-Y. Song *et al.*, "Cross Sections for Electron Collisions with Methane," *Journal of Physical and Chemical Reference Data*, vol. 44, no. 2, May 2015, Art. no. 023101, https://doi.org/10.1063/1.4918630.

[28] W. Sohn, K. Jung, and H. Ehrhardt, "Threshold structures in the cross sections of low-energy electron scattering of methane," *Journal of Physics B Atomic Molecular Physics*, vol. 16, pp. 891–901, Mar. 1983, https://doi.org/10.1088/0022-3700/16/5/020.

[29] R. K. Janev and D. Reiter, "Collision processes of CHy and CHy+ hydrocarbons with plasma electrons and protons," *Physics of Plasmas*, vol. 9, no. 9, pp. 4071–4081, Sep. 2002, https://doi.org/10.1063/1.1500735.

[30] H. Cho *et al.*, "A comparative experimental–theoretical study on elastic electron scattering by methane," *Journal of Physics B: Atomic, Molecular and Optical Physics*, vol. 41, no. 4, Oct. 2008, Art. no. 045203, https://doi.org/10.1088/0953-4075/41/4/045203.

[31] L. Boesten and H. Tanaka, "Elastic DCS for e+CH4 collisions, 1.5-100 eV," *Journal of Physics B: Atomic, Molecular and Optical Physics*, vol. 24, no. 4, Oct. 1991, Art. no. 821, https://doi.org/10.1088/0953-4075/24/4/009.

[32] W. Sohn, K.-H. Kochem, K.-M. Scheuerlein, K. Jung, and H. Ehrhardt, "Elastic electron scattering from CH4 for collision energies between 0.2 and 5 eV," *Journal of Physics B: Atomic and Molecular Physics*, vol. 19, no. 21, Aug. 1986, Art. no. 3625, https://doi.org/10.1088/0022-3700/19/21/024.

[33] I. Iga, M.-T. Lee, M. G. P. Homem, L. E. Machado, and L. M. Brescansin, "Elastic cross sections for e^- - CH_4 collisions at intermediate energies," *Physical Review A*, vol. 61, no. 2, Jan. 2000, Art. no. 022708, https://doi.org/10.1103/PhysRevA.61.022708.

[34] L. Vuškovič and S. Trajmar, "Electron impact excitation of methane," *The Journal of Chemical Physics*, vol. 78, no. 8, pp. 4947–4951, Apr. 1983, https://doi.org/10.1063/1.445405.

[35] H. Tanaka, T. Okada, L. Boesten, T. Suzuki, T. Yamamoto, and M. Kubo, "Differential cross sections for elastic scattering of electrons by CH4 in the energy range of 3 to 20 eV," *Journal of Physics B: Atomic and Molecular Physics*, vol. 15, no. 18, Jun. 1982, Art. no. 3305, https://doi.org/10.1088/0022-3700/15/18/024.

[36] T. W. Shyn and T. E. Cravens, "Angular distribution of electrons elastically scattered from CH4," *Journal of Physics B: Atomic, Molecular and Optical Physics*, vol. 23, no. 2, Jan. 1990, Art. no. 293, https://doi.org/10.1088/0953-4075/23/2/011.

[37] C. T. Bundschu *et al.*, "Low-energy electron scattering from methane," *Journal of Physics B: Atomic, Molecular and Optical Physics*, vol. 30, no. 9, Feb. 1997, Art. no. 2239, https://doi.org/10.1088/0953-4075/30/9/023.

[38] T. W. Shyn, "Vibrational excitation cross sections of methane by electron impact," *Journal of Physics B: Atomic, Molecular and Optical Physics*, vol. 24, no. 24, Sep. 1991, Art. no. 5169, https://doi.org/10.1088/0953-4075/24/24/014.

[39] H. Tanaka, M. Kubo, N. Onodera, and A. Suzuki, "Vibrational excitation of CH4 by electron impact: 3-20 eV," *Journal of Physics B: Atomic and Molecular Physics*, vol. 16, no. 15, Dec. 1983, Art. no. 2861, https://doi.org/10.1088/0022-3700/16/15/026.

[40] W. Sohn, K. Jung, and H. Ehrhardt, "Threshold structures in the cross sections of low-energy electron scattering of methane," *Journal of Physics B: Atomic and Molecular Physics*, vol. 16, no. 5, Nov. 1983, Art. no. 891, https://doi.org/10.1088/0022-3700/16/5/020.

[41] H. C. Straub, D. Lin, B. G. Lindsay, K. A. Smith, and R. F. Stebbings, "Absolute partial cross sections for electron-impact ionization of CH4 from threshold to 1000 eV," *The Journal of Chemical Physics*, vol. 106, no. 11, pp. 4430–4435, Mar. 1997, https://doi.org/10.1063/1.473468.

[42] D. Rapp and P. Englander-Golden, "Total Cross Sections for Ionization and Attachment in Gases by Electron Impact. I. Positive Ionization," *The Journal of Chemical Physics*, vol. 43, no. 5, pp. 1464–1479, Sep. 1965, https://doi.org/10.1063/1.1696957.

[43] M.-Y. Song *et al.*, "Cross Sections for Electron Collisions with Methane," *Journal of Physical and Chemical Reference Data*, vol. 44, no. 2, May 2015, Art. no. 023101, https://doi.org/10.1063/1.4918630.

[44] H. F. Winters, "Dissociation of methane by electron impact," *The Journal of Chemical Physics*, vol. 63, no. 8, pp. 3462–3466, Oct. 1975, https://doi.org/10.1063/1.431783.

[45] S. Motlagh and J. H. Moore, "Cross sections for radicals from electron impact on methane and fluoroalkanes," *The Journal of Chemical Physics*, vol. 109, no. 2, pp. 432–438, Jul. 1998, https://doi.org/10.1063/1.476580.

[46] G. J. M. Hagelaar and L. C. Pitchford, "Solving the Boltzmann equation to obtain electron transport coefficients and rate coefficients for fluid models," *Plasma Sources Science and Technology*, vol. 14, no. 4, Jul. 2005, Art. no. 722, https://doi.org/10.1088/0963-0252/14/4/011.

[47] X. L. Liu and D. M. Xiao, "Monte Carlo simulation of electron swarm parameters in c-C4F8," *The European Physical Journal - Applied Physics*, vol. 38, no. 3, pp. 269–274, Jun. 2007, https://doi.org/10.1051/epjap:2007087.

[48] X. Liu, D. Xiao, Y. Wang, and Z. Zhang, "Monte Carlo simulation of electron swarms parameters in c-C4F8/CF4 gas mixtures," *Journal of Shanghai Jiaotong University (Science)*, vol. 13, no. 4, pp. 443–447, Aug. 2008, https://doi.org/10.1007/s12204-008-0443-7.